The crystal structure of the Shetha Protein II (FeSII) from *Azotobacter vinelandii* suggests a domain swap

Burak V. Kabasakal[a,b], Ciaran R. Mcfarlane[a], Charles A. R. Cotton[a,c], Anna Schmidt[a], Andrea Kung[a], Lucas Lieber[a,d] and James W. Murray[a**]

a Department of Life Sciences, Imperial College, London, London SW7 2AZ, United Kingdom
b Turkish Accelerator and Radiation Laboratory, Gőlbaşı, 06830, Ankara, Turkiye
c Cambrium GmbH, Max-Urich-Strasse 3, 13355, Berlin, Germany
d Bioheuris Inc. 1100 Corporate Square Dr, St. Louis, MO 63132 USA
** to whom correspondence should be addressed. Email: j.w.murray@imperial.ac.uk

keywords: nitrogen fixation, oxygen protection, structural biology, domain swap

ABSTRACT

The *Azotobacter vinelandii* FeSII protein forms an oxygen resistant complex with the nitrogenase MoFe and Fe proteins. FeSII is an adrenodoxin type ferredoxin, forming a dimer in solution. Previously, the crystal structure was solved (Schlesier et al., 2016), with 5 copies in the asymmetric unit. One copy is a normal adrenodoxin domain, forming a dimer with its crystallographic symmetry mate. The other four copies are in an “open” conformation with a loop flipped out exposing the 2Fe-2S cluster. The open and closed conformations were interpreted as oxidised and reduced, and the large conformational change in the open configuration allowed binding to nitrogenase. We have independently solved the structure of FeSII in the same crystal form. Our positioning of the atoms in the unit cell is similar to the earlier report. However, our interpretation of the structure is different. We interpret the “open” conformation as the product of a crystallization-induced domain swap. The 2Fe-2S cluster is not exposed to solvent, but in the crystal its interacting helix is replaced by the same helix residues from a crystal symmetry mate. The domain swap is complicated, as it is unusual in being in the middle of the protein rather than at a terminus, and it creates arrangements of molecules that can be interpreted in multiple ways. We caution that crystal structures should be interpreted in terms of the contents of the entire crystal rather than one asymmetric unit.

Introduction

Nitrogen is an essential component of DNA and proteins. Nitrogen gas makes up 80% of the atmosphere, but it is very unreactive. Fixing this unreactive nitrogen is an essential biological and industrial process. Biological nitrogen fixation is catalysed by the enzyme nitrogenase, which reduces nitrogen gas to ammonia. The nitrogen reduction is catalysed by the MoFe protein, a $(NifDNifK)_2$ tetramer, containing molybdenum. The MoFe protein is in turn reduced by the dinitrogenase reductase, the Fe protein, a dimer of NifH. MoFe has two oxygen sensitive metalloclusters, the P-cluster and the FeMoCo, containing the molybdenum atom. The Fe protein has a low potential 4Fe-4S cluster at the surface bridging the dimer interface. Both nitrogenase components are irreversibly inhibited by oxygen, which reacts with the low potential iron-sulfur clusters. MoFe has a half life of around 10 minutes in air, and the Fe protein has a half life of around 45 seconds (Robson, 1979; Robson and Postgate, 1980). The MoFe:Fe protein complex is partially protected from oxygen, relative to each protein individually (Schlesier et al., 2016). As well as direct inactivation of the nitrogenase, oxygen reactions with nitrogenase proteins probably generate damaging reactive oxygen species (Maier and Moshiri, 2000).

Organisms that fix nitrogen, known as diazotrophs, use several strategies to protect themselves from oxygen. Some are obligate anaerobes or micro-aerobes. Some diazotrophic aerobes such as *Azotobacter* species use “respiratory protection”, a fast respiratory rate to consume oxygen. A second mechanism is “conformational protection”. It was noticed that a nitrogen fixing culture of *Azotobacter chroococcum* would stop fixing oxygenated by strong agitation, but when the agitation stopped, the culture would resume nitrogen fixation at the same rate as before (Hill et al., 1972). This result implied that the nitrogenase was being temporarily inactivated, by a “conformational” mechanism.

In the 1960s, Shethna and colleagues isolated several non-heme iron proteins from *Azotobacter vinelandii* (Shethna et al., 1968). The second of these proteins became known as the Shethna protein, or FeSII. Early work on purifying nitrogenase found a pink protein that associated with nitrogenase, and provided some oxygen protection (Kelly et al., 1967). This pink protein was then identified as the FeSII protein (Bulen and LeComte, 1972; Haaker and Veeger, 1977). FeSII is the basis of the conformational protection (Robson, 1979). It forms a ternary complex with the MoFe and Fe proteins that is catalytically inactive, but from which active nitrogenase can be recovered, with a half life in air of about an hour (Robson, 1979). FeSII is not essential for *A. vinelandii* viability, even under nitrogen fixing conditions, but the nitrogenase was more sensitive to inactivation in an FeSII knockout mutant (Moshiri et al., 1994).

FeSII has only been shown to have protective activity in *A. vinelandii and A. chroococcum*, although FeSII-like functionality has been proposed for other ferredoxins associated with nitrogenase operons, for example FdxD in *Rhodobacter capsulatus* (Hoffmann et al., 2014) and a *Guconacetobacter* ferredoxin (Lery et al., 2010; Ureta and Nordlund, 2002). It is possible that protective function has appeared more than once, or that similar mechanisms exist in other diazotrophs, but have not yet been identified.

FeSII is a 13 kDa adrenodoxin type ferredoxin protein with a 2Fe-2S cluster, forming a dimer in solution, the midpoint potential is -262 mV (Moshiri et al., 1995). The crystallization was published in 1995 (Moshiri et al., 1995), in an orthorhombic crystal form, but no structure was solved. Recently Schlesier *et al* (Schlesier et al., 2016) reported a 2.2 Å crystal structure of FeSII in the same orthorhombic crystal form. The observed FeSII crystal form has five copies in the asymmetric unit. One of them is in a “closed conformation”, forming a “closed” dimer with a crystallographic symmetry mate. The closed conformation is similar other adrenodoxin proteins, such as the monomeric *E. coli* Fdx (Kakuta et al., 2001). The other four copies in the asymmetric unit are in an “open” from. In the open form, the so-called N-loop from residues 59-96 is flipped out from the structure so that the 2Fe-2S cluster is revealed. Specifically, the “lid helix” from residues 68-78 is moved away from the cluster. The four open FeSII were interpreted as two dimers of the same type as the closed form, but with the N-loop flipped out. Schlesier et al proposed that this conformational change is triggered by oxidation of the cluster, and the change enables FeSII to form the protective ternary complex with MoFe and Fe proteins. The open form of FeSII has not been observed in crystals of any other adrenodoxin type domains.

Protein domain swapping is when two protein molecules exchange equivalent regions in their structures (Liu and Eisenberg, 2002; Wodak et al., 2015). In the simplest form, two adjacent monomers swap a region to form a domain-swapped dimer. Some proteins have evolved natural domain swaps, relative to an unswapped ancestor (Cahyono et al., 2020). In other cases the swap is functional, or may be involved in disease (Rousseau et al., 2012). Domain swapping may also be induced by chemical treatment (Cahyono et al., 2020) or crystallization. For example in a crystallised PAS domain, one of the six non-

crystallographic symmetry copies had a domain-swapped C-terminal alpha-helix (Emami et al., 2009). In cyanobacterial Psb29 (Bečková et al., 2017), only one of three crystal forms had a domain-swapped N-terminal alpha-helix (Bečková et al., 2017). In these cases, the domain swapped structure may be regarded as a crystallization artefact, and the swapped structure is not biologically relevant. In most domain-swapped structures the swap is of one end of the structure containing the N- and C-terminus. Swaps of internal regions are rarer, but have been observed, such as in the structure of IX/X-binding protein from snake venom (Mizuno et al., 1997), which has a loop exchange heterodimer, relative to a the homologous rat mannose binding protein (Weis et al., 1991).

We have independently solved the structure of the FeSII protein in the same crystal form as previously, to higher resolution. Our atoms are in similar positions to the earlier structure, but our interpretation of the open form of the protein is very different. We believe that the open form is caused by a crystallization-induced domain swap. Here, we present evidence that the "open" conformation of FeSII in the crystal structure is best interpreted as a domain-swapped structure.

Results

FeSII structure

We independently solved the FeSII structure using Fe-SAD to a final resolution of 1.65 Å in the same orthorhombic $P2_12_12$ crystal form as observed in 1995 (Moshiri et al., 1995) and 2016 (Schlesier et al., 2016). Data and refinement information are in Table S1. The asymmetric unit contains five copies of FeSII. One is in the closed conformation similar to other adrenodoxins. The other four are in the open conformation. Although the crystal form is the same, we have placed the open protein chains in different symmetry positions to highlight our interpretation of the structure. The structures are similar, with an RMSD of 1.1 Å over the closed chain between this work and Schlesier et al (2016), and 0.4 Å between the best matching open chains. The closed chain is more complete than before, with a gap from residues 82-92 in the N-loop. In the open chains, the N-loop is ordered, and the entire chain is visible, apart from the N- and C-termini.

Interpretation of crystal structure

In this crystal form the "closed" chain E forms a dimer with its crystallographic symmetry mate E' (-X+1, -Y, Z). All four open chains form the "open dimer". Chains A and B form this dimer. Chain C forms this dimer with Chain D from the X,Y,Z-1 symmetry mate (D'). Chains C and D form another extended interface forming we call the "domain-swap" dimer. Chain A also forms this domain swap dimer with the B chain related by X,Y,Z-1 (B'). All open chains are involved in both the "open" and "domain-swap" dimers. Fig 1 shows the dimers in the crystal and the chains forming them for two unit cells.

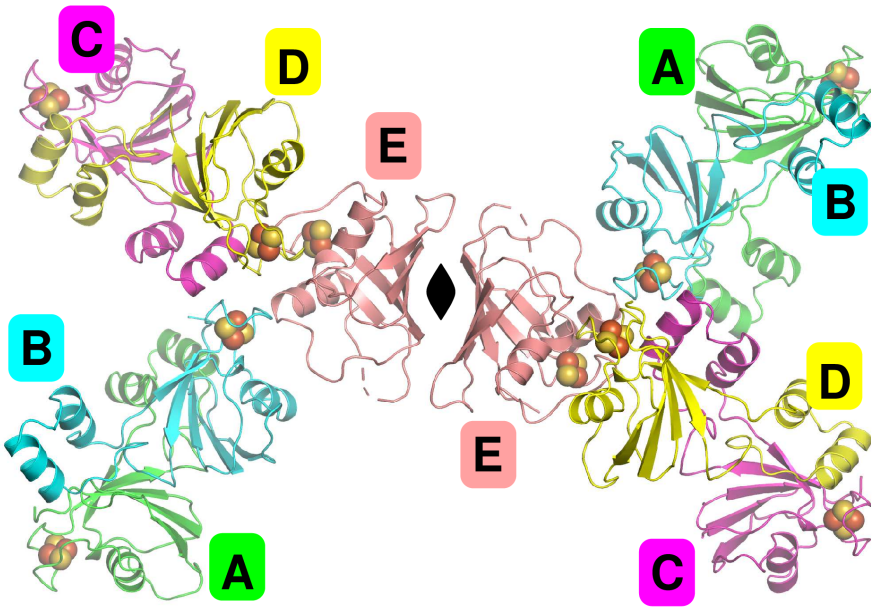

Figure 1: The contents of two unit cells of the FeSII protein, showing the five unique chains A, B, C, D.

The work by Schlesier et al proposed that the "lid helix", moves away from the 2Fe-2S cluster in the open dimer, exposing it to solvent. However, in the crystal, in each open chain the lid helix is replaced by a lid helix from a symmetry related chain. Fig. 2a shows the lid helix in place for chain E, the closed chain. For the open chain C, Fig. 2b shows the lid helix in an equivalent position, but coming from the domain-swap dimer partner chain D in the crystal. In chains A and B, the lid helix is similarly replaced by symmetry related chains B' and A' respectively.

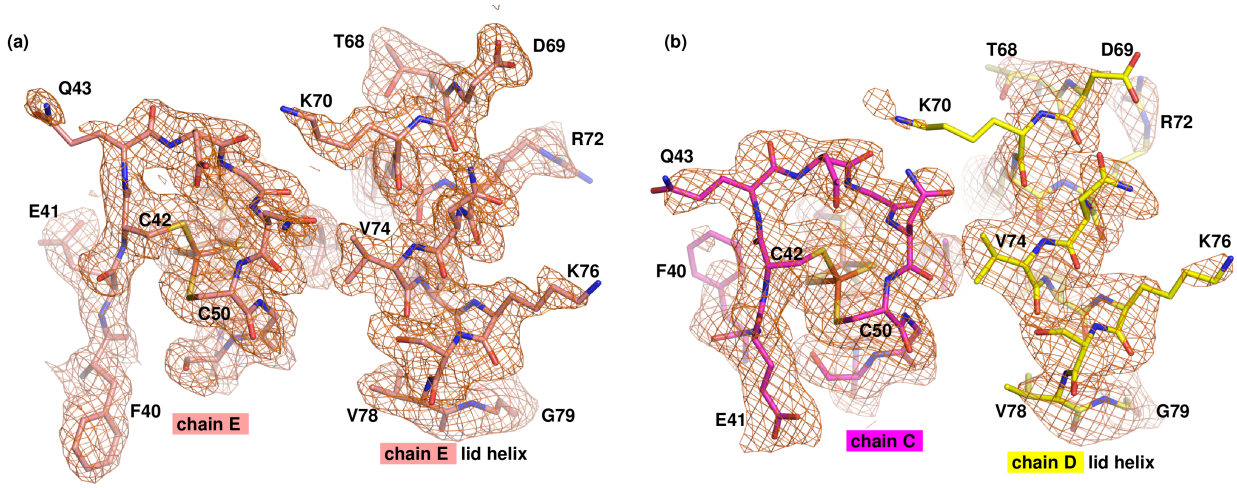

Figure 2: Region around the 2Fe-2S cluster for closed and open chains. For chain E (salmon) in the crystal, the lid helix from chain E covers the iron-sulfur cluster. For chain C (magenta), the lid helix is flipped out in the open conformation, but the cluster is still capped by the lid helix from chain D. Weighted $2F_o$-F_c density is contoured at 0.9σ and selected residues are labelled.]

The predicted interface areas, and binding energies for the dimers that exist in the crystal are shown in Table 1. The calculated area of the closed dimer interface is 490 $Å^2$.
In the open conformation, the "lid helix" (residues 68-79), as part of the longer "N-loop" (residues 59-96) is folded away from the central domain. It forms additional contacts with

the closed dimer partner around Pro12, expanding the closed dimer interface. The calculated area of the closed dimer interface is 490 Å^2, but the mean open dimer interface area is 1120 Å^2. In the crystal, the open dimers are also involved in the domain swap dimer. This dimer is interface is primarily made up of residues of the opened out N-loop, but has a mean area of 970 Å^2, and is the most energetically favoured of the interfaces. These predicted energies suggest that the formation of the open and domain swap interfaces is energetically favoured in the crystal.

Interface	Chains	Interface Area / Å^2	Predicted binding energy / kcal mol^{-1}
OPEN 1	A:B	1170	-9.3
OPEN 2	C:D' [X,Y,Z-1]	1080	-8.4
MEAN OPEN	A:B, C:D'	1120	-8.9
DOMAIN SWAP 1	C:D	983	-16.6
DOMAIN SWAP 2	A:B' [X, Y, Z-1]	960	-17.0
MEAN DOMAIN SWAP	C:D, A:B'	970	-16.8
CLOSED	E:E' [-X+1, -Y,Z]	490	-4.8

Table 1: Interface areas in Å^2, calculated as half the difference in total accessible surface areas of isolated and interfacing structures.

The dimers in the FeSII crystal are shown in Fig. 3 in cartoon and schematic view.The replacement of the lid helix by the lid helix from a symmetry mate (red in Fig 3), may be interpreted as a domain swap of the N-loop. This domain swap is unusual in that it involves an internal region of the protein rather than an N- or C-terminus. The swap is also unusual in that it creates an extensive new dimer interface, in addition to the dimer interface that is present in the open and closed dimers. Given that these two interfaces can only occur together in the crystal, we suggest that this open conformation of FeSII is crystallization induced. The flexibility of the "hinge" regions proposed earlier may allow this protein to change shape under the constraints of crystal lattice formation to a more energetically favoured conformation that may not be biologically relevant.

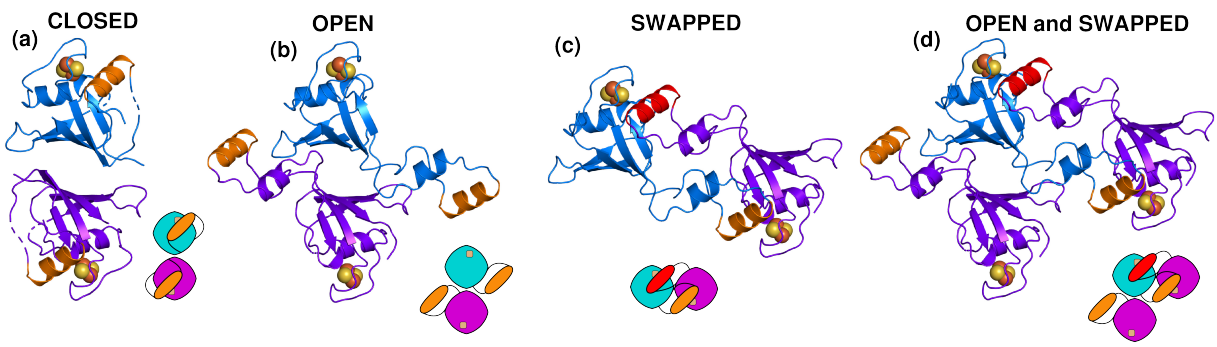

Figure 3: Cartoon and schematic view of the dimers of FeSII in the P21212 FeSII crystal form. (a) closed dimer (chains E and E'), (b) open dimer (chains A and B) (c) domain swap dimer (chains A and B'). (d) Open and domain swap dimers (A, B and B')
The chains are shown in blue and purple, with the lid helix (residues 68-79) in orange, except for the top lid helix when interpreted as part of the domain swap dimer, when it is shown in red.

Schlesier et al propose that the formation of the open dimers is induced by the oxidation of the 2Fe-2S cluster. Our protein and crystals were prepared aerobically, and our protein has an absorption spectrum corresponding to oxidised protein (Fig S1) so even the closed chain should be oxidised, and so any conformational change is not driven by differential oxidation states of the 2Fe-2S cluster.

Discussion

Previous research has claimed that the FeSII protein adopts a radically changed conformation in the oxidised state, based on the crystal structure and small shifts in retention time in size-exclusion chromatography. We have independently solved the FeSII crystal structure at 1.65 Å resolution. Based on examination of the full unit cell of the crystal, we conclude that the "open" structure seen in the crystal is most likely due to crystallization-induced domain-swapping. Previous work on the homologous ferredoxin VI from *Rhodobacter capsulatus* (Sainz et al., 2006) solved structures of the oxidised and reduced protein (Armengaud et al., 2001; Sainz et al., 2006) and only small conformational changes were seen, mainly around the iron-sulfur cluster. It is likely that the interaction of FeSII with nitrogenase is also governed by only small conformational changes. We await structure determination of the full MoFe:Fe:FeSII protein complex for confirmation.

Materials and Methods

Overexpression and Purification of FeSII

A synthetic gene coding for the FeSII from *Azotobacter vinelandii* (AVIN_39700) was synthesised by DNA 2.0 (California, USA), and sub-cloned into a pRSET-A vector (Invitrogen, Carlsbad, CA, USA) with no tag. The FeSII gene was PCR amplified with primers FESII_FOR 5'-TATTACATATGGCGACGATCTATTTCAGCAGC-3' and FESII_REV 5'-ATTATCTCGAGTTATCAGGCGCCACCCG-3' (restriction sites underlined) and the product digested with NdeI and XhoI, and then ligated into vector cut with NdeI and XhoI restriction enzymes.
FeSII protein was produced by transformation of the vector into chemically competent *E. coli* KRX cells (Promega, Wisconsin, USA), and cultivation in 1 L Terrific Broth medium supplemented with 100 µg/l ampicillin. Expression was induced at an OD600 of 0.6-0.8 with 1 g/l L-rhamnose monohydrate. After overnight induction at 18° C, the cells were harvested by centrifugation, and resuspended in 10 mM HEPES pH 7.4, 1 mM $MgCl_2$. Cell disruption was performed by sonication. FeSII was purified with a modification of a published method (Moshiri et al., 1995). 0.4 % (w/v) NaCl and 11% (w/v) PEG 8000 were added as powder to the lysate. They were mixed gently for 45 min at 4°C, and the cell debris was separated by centrifugation. The red supernatant was filtered through a 0.2 µm filter, and purified by anion exchange chromatography on a Q Sepharose column equilibrated against 10 mM HEPES, pH 7.4, 1 mM $MgCl_2$. FeSII was eluted by using a linear gradient of $MgCl_2$ from 0 mM to 50 mM over 10 column volumes. The fractions corresponding to FeSII protein were pooled and concentrated, and further purified by size-exclusion chromatography (HiLoad 16/600 Superdex 200 PG column) in 10 mM HEPES, pH 7.4, 5 mM MgCl2, 100 mM NaCl.

Structure Determination of FeSII

FeSII was crystallized using hanging drop vapor diffusion with an equal mix of 0.1 M HEPES pH 8.0, 0.2 M sodium citrate, 24%, (w/v) PEG3350, 2% (v/v) 1-butanol and

40 mg/ml FeSII. Crystals were cryoprotected for 30 s in the mother liquor solution with 30% volume added PEG400, and flash cooled in liquid nitrogen. X-ray diffraction data were collected at 100 K on beamline I03 at Diamond Light Source, UK. For phase determination, a data set was collected at the iron K-edge at a wavelength of 1.734 Å. The data were processed and scaled with xia2 (Winter, 2010) and XDS (Kabsch, 2010). The structure was phased with Fe-SAD using the intrinsic Fe atoms of the protein using AutoSol of the phenix package. Phases were improved with density modification in DM (Cowtan, 2010), and a preliminary model built with Buccaneer (Cowtan, 2006). The model was rebuilt manually in Coot (Emsley et al., 2010), cycling with refinement in phenix.refine (Adams et al., 2010). This model was then refined and rebuilt against a higher resolution native dataset at 1.65 Å. The structure was validated with MolProbity (Williams et al., 2018). Final data collection and refinement statistics are given in Supporting Table 1. Dimer surface areas and interaction energies were predicted with PISA (Krissinel, 2010; Krissinel and Henrick, 2007). Molecular figures were produced in PyMol (Delano, 2002).

Acknowledgements: The authors would like to thank Diamond Light Source for beam time (proposal mx12579), and the staff of beam lines I02, I03 and I24 for assistance with crystal testing and data collection. This work was funded in part by the BBSRC/NSF Nitrogen Ideas Lab: Oxygen-Tolerant Nitrogenase (BB/L011468/1). The crystallization facility at Imperial College was funded by BBSRC (BB/D524840/1) and the Wellcome Trust (202926/Z/16/Z). CRM was funded by a BBSRC Doctoral Training Programme (BB/J014575/1), as was CARC (BB/F017324/1).

Conflict of Interest: The authors declare that they have no conflicts of interest with the contents of this article.

Author contributions: JWM, LL, CARC, AK, AS, CRM, BVK, performed research. JWM drafted the paper in consultation with the other authors.

REFERENCES

Adams, P.D., Afonine, P.V., Bunkóczi, G., Chen, V.B., Davis, I.W., Echols, N., Headd, J.J., Hung, L.W., Kapral, G.J., Grosse Kunstleve, R.W., McCoy, A.J., Moriarty, N.W., Oeffner, R., Read, R.J., Richardson, D.C., Richardson, J.S., Terwilliger, T.C., Zwart, P.H., 2010. PHENIX: a comprehensive Python-based system for macromolecular structure solution. Acta Crystallogr. D Biol. Crystallogr. 66, 213–221. https://doi.org/10.1107/s0907444909052925

Armengaud, J., Sainz, G., Jouanneau, Y., Sieker, L.C., 2001. Crystallization and preliminary X-ray diffraction analysis of a [2Fe–2S] ferredoxin (FdVI) from Rhodobacter capsulatus. Acta Crystallogr. D Biol. Crystallogr. 57, 301–303. https://doi.org/10.1107/S0907444900017832

Bečková, M., Yu, J., Krynická, V., Kozlo, A., Shao, S., Koník, P., Komenda, J., Murray, J.W., Nixon, P.J., 2017. Structure of Psb29/Thf1 and its association with the FtsH protease complex involved in photosystem II repair in cyanobacteria. Phil Trans R Soc B 372, 20160394+. https://doi.org/10.1098/rstb.2016.0394

Beitz, E., 2000. TeXshade: shading and labeling of multiple sequence alignments using LaTeX2e. Bioinforma. Oxf. Engl. 16, 135–139. https://doi.org/10.1093/bioinformatics/16.2.135

Bulen, W.A., LeComte, J.R., 1972. Nitrogenase complex and its components. Methods Enzymol. 24, 456–470.

Cahyono, R.N., Yamanaka, M., Nagao, S., Shibata, N., Higuchi, Y., Hirota, S., 2020. 3D domain swapping of azurin from *Alcaligenes xylosoxidans*. Metallomics. https://doi.org/10.1039/C9MT00255C
Cowtan, K., 2010. Recent developments in classical density modification. Acta Crystallogr. D Biol. Crystallogr. 66, 470–478. https://doi.org/10.1107/s090744490903947x
Cowtan, K., 2006. The Buccaneer software for automated model building. 1. Tracing protein chains. Acta Crystallogr. D Biol. Crystallogr. 62, 1002–1011. https://doi.org/10.1107/s0907444906022116
Delano, W.L., 2002. The PyMOL Molecular Graphics System. DeLano Scientific, Palo Alto, CA, USA.
Emami, K., Topakas, E., Nagy, T., Henshaw, J., Jackson, K.A., Nelson, K.E., Mongodin, E.F., Murray, J.W., Lewis, R.J., Gilbert, H.J., 2009. Regulation of the xylan-degrading apparatus of *Cellvibrio japonicus* by a novel two-component system. J. Biol. Chem. 284, 1086–1096. https://doi.org/10.1074/jbc.m805100200
Emsley, P., Lohkamp, B., Scott, W.G., Cowtan, K., 2010. Features and development of Coot. Acta Crystallogr. D Biol. Crystallogr. 66, 486–501. https://doi.org/10.1107/s0907444910007493
Haaker, H., Veeger, C., 1977. Involvement of the cytoplasmic membrane in nitrogen fixation by *Azotobacter vinelandii*. Eur. J. Biochem. 77, 1–10. https://doi.org/10.1111/j.1432-1033.1977.tb11634.x
Hill, S., Drozd, J.W., Postgate, J.R., 1972. Environmental effects on the growth of nitrogen-fixing bacteria. J Appl Chem 22, 541–558. https://doi.org/10.1002/jctb.2720220413
Hoffmann, M.-C.C., Müller, A., Fehringer, M., Pfänder, Y., Narberhaus, F., Masepohl, B., 2014. Coordinated expression of *fdxD* and molybdenum nitrogenase genes promotes nitrogen fixation by *Rhodobacter capsulatus* in the presence of oxygen. J. Bacteriol. 196, 633–640. https://doi.org/10.1128/jb.01235-13
Kabsch, W., 2010. Integration, scaling, space-group assignment and post-refinement. Acta Crystallogr. D Biol. Crystallogr. 66, 133–144. https://doi.org/10.1107/s0907444909047374
Kakuta, Y., Horio, T., Takahashi, Y., Fukuyama, K., 2001. Crystal structure of *Escherichia coli* Fdx, an adrenodoxin-type ferredoxin involved in the assembly of iron-sulfur clusters. Biochemistry 40, 11007–11012.
Kelly, M., Klucas, R.V., Burris, R.H., 1967. Fractionation and storage of nitrogenase from *Azotobacter vinelandii*. Biochem. J. 105, 3C-5C. https://doi.org/10.1042/bj1050003c
Krissinel, E., 2010. Crystal contacts as nature's docking solutions. J. Comput. Chem. 31, 133–143. https://doi.org/10.1002/jcc.21303
Krissinel, E., Henrick, K., 2007. Inference of macromolecular assemblies from crystalline state. J. Mol. Biol. 372, 774–797. https://doi.org/10.1016/j.jmb.2007.05.022
Lery, L.M., Bitar, M., Costa, M.G., Rössle, S.C., Bisch, P.M., 2010. Unraveling the molecular mechanisms of nitrogenase conformational protection against oxygen in diazotrophic bacteria. BMC Genomics 11 Suppl 5. https://doi.org/10.1186/1471-2164-11-s5-s7
Liu, Y., Eisenberg, D., 2002. 3D domain swapping: as domains continue to swap. Protein Sci. Publ. Protein Soc. 11, 1285–1299. https://doi.org/10.1110/ps.0201402
Lou, J., Moshiri, F., Johnson, M.K., Lafferty, M.E., Sorkin, D.L., Miller, A., Maier, R.J., 1999. Mutagenesis studies of the FeSII protein of *Azotobacter vinelandii*: roles of histidine and lysine residues in the protection of nitrogenase from oxygen damage. Biochemistry 38, 5563–5571. https://doi.org/10.1021/bi9827823
Maier, R.J., Moshiri, F., 2000. Role of the *Azotobacter vinelandii* nitrogenase-protective shethna protein in preventing oxygen-mediated cell death. J. Bacteriol. 182, 3854–3857.

Mizuno, H., Fujimoto, Z., Koizumi, M., Kano, H., Atoda, H., Morita, T., 1997. Structure of coagulation factors IX/X-binding protein, a heterodimer of C-type lectin domains. Nat. Struct. Biol. 4, 438–441.

Moshiri, F., Crouse, B.R., Johnson, M.K., Maier, R.J., 1995. The “nitrogenase-protective” FeSII protein of *Azotobacter vinelandii*: overexpression, characterization, and crystallization. Biochemistry 34, 12973–12982. https://doi.org/10.1021/bi00040a007

Moshiri, F., Kim, J.W., Fu, C., Maier, R.J., 1994. The FeSII protein of *Azotobacter vinelandii* is not essential for aerobic nitrogen fixation, but confers significant protection to oxygen-mediated inactivation of nitrogenase in vitro and in vivo. Mol. Microbiol. 14, 101–114.

Robson, R.L., 1979. Characterization of an oxygen-stable nitrogenase complex isolated from *Azotobacter chroococcum*. Biochem. J. 181, 569–575.

Robson, R.L., Postgate, J.R., 1980. Oxygen and hydrogen in biological nitrogen fixation. Annu. Rev. Microbiol. 34, 183–207.

Rousseau, F., Schymkowitz, J., Itzhaki, L.S., 2012. Implications of 3D Domain Swapping for Protein Folding, Misfolding and Function, in: Matthews, J.M. (Ed.), Protein Dimerization and Oligomerization in Biology. Springer New York, New York, NY, pp. 137–152. https://doi.org/10.1007/978-1-4614-3229-6_9

Sainz, G., Jakoncic, J., Sieker, L.C., Stojanoff, V., Sanishvili, N., Asso, M., Bertrand, P., Armengaud, J., Jouanneau, Y., 2006. Structure of a [2Fe–2S] ferredoxin from *Rhodobacter capsulatus* likely involved in Fe–S cluster biogenesis and conformational changes observed upon reduction. JBIC J. Biol. Inorg. Chem. 11, 235–246. https://doi.org/10.1007/s00775-005-0069-2

Schlesier, J., Rohde, M., Gerhardt, S., Einsle, O., 2016. A Conformational Switch Triggers Nitrogenase Protection from Oxygen Damage by Shethna Protein II (FeSII). J. Am. Chem. Soc. 138, 239–247.

Shethna, Y.I., DerVartanian, D.V., Beinert, H., 1968. Non heme (iron-sulfur) proteins of *Azotobacter vinelandii*. Biochem. Biophys. Res. Commun. 31, 862–868. https://doi.org/10.1016/0006-291x(68)90531-7

Ureta, A., Nordlund, S., 2002. Evidence for conformational protection of nitrogenase against oxygen in Gluconacetobacter diazotrophicus by a putative FeSII protein. J. Bacteriol. 184, 5805–5809. https://doi.org/10.1128/jb.184.20.5805-5809.2002

Weis, W.I., Kahn, R., Fourme, R., Drickamer, K., Hendrickson, W.A., 1991. Structure of the Calcium-Dependent Lectin Domain from a Rat Mannose-Binding Protein Determined by MAD Phasing. Science 254, 1608–1615. https://doi.org/10.1126/science.1721241

Williams, C.J., Headd, J.J., Moriarty, N.W., Prisant, M.G., Videau, L.L., Deis, L.N., Verma, V., Keedy, D.A., Hintze, B.J., Chen, V.B., Jain, S., Lewis, S.M., Arendall, W.B., Snoeyink, J., Adams, P.D., Lovell, S.C., Richardson, J.S., Richardson, D.C., 2018. MolProbity: More and better reference data for improved all-atom structure validation. Protein Sci. Publ. Protein Soc. 27, 293–315.

Winter, G., 2010. *xia2*: an expert system for macromolecular crystallography data reduction. J Appl Cryst 43, 186–190.

Wodak, S.J., Malevanets, A., MacKinnon, S.S., 2015. The Landscape of Intertwined Associations in Homooligomeric Proteins. Biophys. J. 109, 1087–1100. https://doi.org/10.1016/j.bpj.2015.08.010

SUPPLEMENTARY INFORMATION

The crystal structure of the Shetha Protein II (FeSII) from *Azotobacter vinelandii* suggests a domain swap

Burak V. Kabasakal[a,b], Ciaran R. Mcfarlane[a], Charles A. R. Cotton[a,c], Anna Schmidt[a], Andrea Kung[a], Lucas Lieber[a] and James W. Murray[a**]

a Department of Life Sciences, Imperial College, London, London SW7 2AZ, United Kingdom
b Turkish Accelerator and Radiation Laboratory, Gőlbaşı, 06830, Ankara, Turkiye
c Cambrium GmbH, Max-Urich-Strasse 3, 13355, Berlin, Germany
** to whom correspondence should be addressed. Email: j.w.murray@imperial.ac.uk

Table S1. FeSII Data collection and refinement statistics. Statistics for the highest-resolution shell are shown in parentheses.

	FeSII (6YAV)
Beamline	I03 Diamond Light Source
Wavelength	0.9763
Resolution range (Å)	37.3 - 1.65 (1.709 - 1.65)
Space group	$P2_12_12$
Unit cell	134.24 Å, 135.1 Å, 37.09 Å, 90°, 90°, 90°
Total reflections	536342 (50652)
Unique reflections	81089 (7901)
Multiplicity	6.6 (6.4)
Completeness (%)	98.33 (97.17)
Mean I/sigma(I)	17.46 (1.47)
Wilson B-factor	32.31
R-merge	0.04731 (1.206)
R-meas	0.0515 (1.313)
R-pim	0.02007 (0.513)
$CC_{1/2}$	0.999 (0.568)
CC*	1 (0.851)
Reflections used in refinement	81085 (7901)
Reflections used for R-free	4037 (380)
R-work	0.1979 (0.3162)
R-free	0.2249 (0.3187)
CC(work)	0.966 (0.754)
CC(free)	0.960 (0.759)
Number of non-hydrogen atoms	4656
macromolecules	4427
ligands	33
solvent	196
Protein residues	590
RMS (bonds)	0.008
RMS (angles)	1.19
Ramachandran favored (%)	98.60
Ramachandran allowed (%)	1.40
Ramachandran outliers (%)	0.00
Rotamer outliers (%)	0.00
Clashscore	2.46
Average B-factor	53.36
macromolecules	53.66
ligands	47.41

solvent	47.75
Number of TLS groups	32
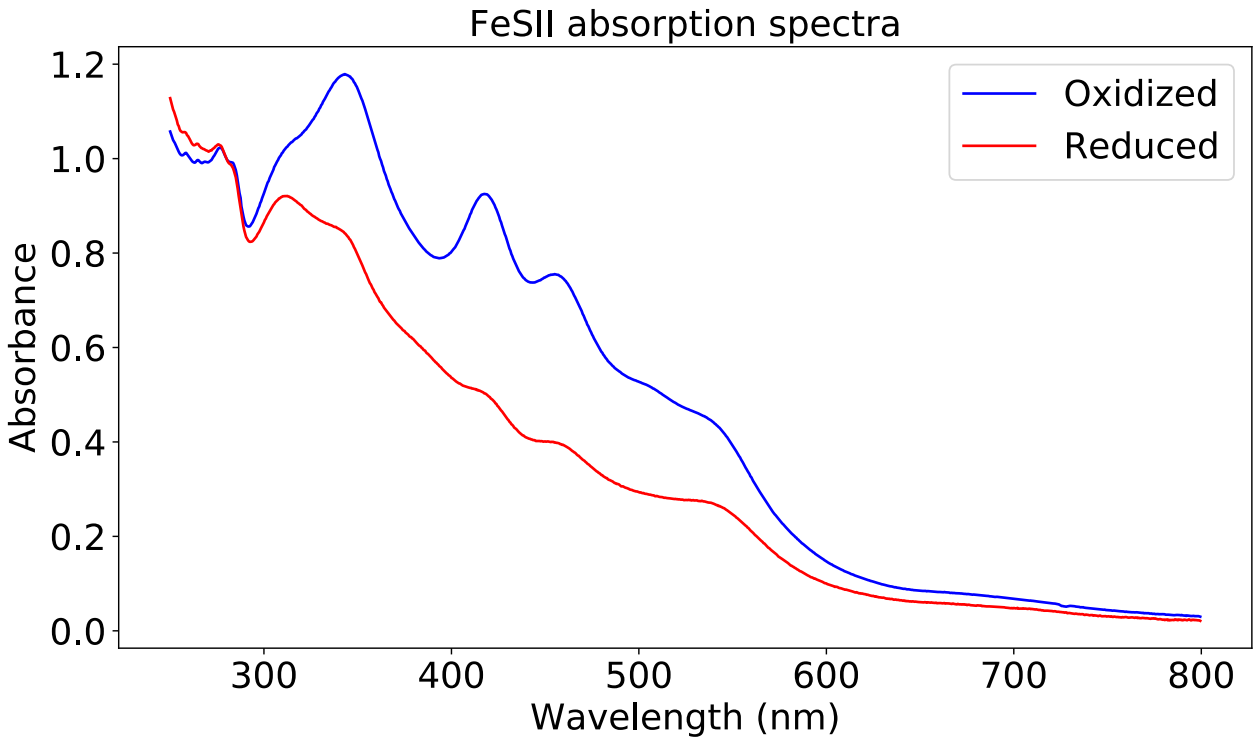
Figure S1. UV-VIS Absorption spectrum of FeSII (1.35 mg/ml) oxidised (blue) and reduced (red) 100 mM HEPES pHh 7.4, 5 mM MgCl2, 100 mM NaCl pH 7.4. Oxidised protein was FeSII prepared in air, reduced protein was prepared by treating anaerobically with 100 µM mM final concentrationsodium dithionite, with excess dithionite removed by repeated centrifugal concentration with a 10 kDa cutoff membrane.